# A Historical Review of Inflatable Aerodynamic Decelerator Technology Development

Brandon P. Smith, Christopher L. Tanner, Milad Mahzari, Ian G. Clark, Robert D. Braun
Daniel Guggenheim School of Aerospace Engineering
Georgia Institute of Technology
Atlanta, GA 30332-0150
404-894-7783
bpsmith@gatech.edu

F. McNeil Cheatwood
NASA Langley Research Center
Hampton, VA 23681

*Abstract*— Viking-era deployable decelerator technology has been employed for several planetary probe missions at Earth and within other planetary atmospheres.[1] [2] Numerous system studies in the past fifty years demonstrate the benefit of developing a new decelerator technology capable of operating at higher Mach numbers and higher dynamic pressures than existing decelerators allow. The deployable Inflatable Aerodynamic Decelerator (IAD) is one such technology. This survey paper describes the development history of the IAD from its conception in the 1960's to the present day. Major findings in primary IAD sub-disciplines for the foremost configurations are discussed. Quantitative engineering data from prior testing is reproduced directly, while qualitative conclusions are referenced in the literature. This work provides a summary of past and present IAD technology development efforts and shows data in a manner useful for today's mission designers.

### TABLE OF CONTENTS



## 1. INTRODUCTION

Cruz [1] defines an IAD as an inflatable device designed to greatly increase drag on an entry vehicle. Its shape is maintained by a mostly closed gas-pressurized three-dimensional body, and is inflated by an internal gas-generating source, ram-air, or both. Nearly five decades have passed since the National Aeronautics and Space Administration (NASA) first proposed use of IAD technology for use of on planetary entry vehicles. This paper surveys the history of IAD technology development and presents the major disciplinary and systems findings for preferred configurations in a manner useful to today's mission designers.

Recent conceptual design studies [1]-[10] emphasize the limitations of the Disk-Gap-Band (DGB) parachute and have sparked renewed interest in the IAD as a mission-enabling technology, but a knowledge gap spanning nearly three decades hinders expedient IAD maturation. Present-day IAD maturation efforts focus on two Viking-era attached IAD configurations, the isotensoid and the tension cone, and one new configuration, the stacked toroid blunted cone. Notional depictions of the favored configurations are shown in Figure 1 along with other tested configurations. The IAD configurations are named for their construction method (stacked toroid) or for the structural theories by which the shapes are derived (isotensoid, tension cone). The primary goal of this survey is to aggregate the documented test data and scientific findings from the aforementioned IAD configurations. Discussions include IAD development history, aerodynamics, static and dynamic stability, aerothermodynamic loading, structural analysis and testing, inflation, and materials.

It is appropriate at this point to define the two most general types of IADs: Supersonic IADs (SIAD) and Hypersonic IADs (HIAD). SIADs are defined as those inflated at supersonic speeds ($M \leq 5$); can use an internal gas source, ram-air, or a combination of both for inflation; must be capable of sustaining moderate levels of heating; and must be capable of deploying and inflating at supersonic Mach numbers against moderate to high dynamic pressures [1]. HIADs are defined as those inflated at hypersonic speeds ($M > 5$) or exo-atmospherically; can be used for aerocapture or entry to landing; and must survive high heating. Many other phrases have been used in the past to describe specific configurations of IADs ("Ballutes", "expandable terminal decelerators", "aerocapture inflatable decelerators", etc.). Recent literature has shied away from such terminology to describe IADs.

[1] 978-1-4244-3888-4/10/$25.00 ©2010 IEEE.
[2] IEEEAC paper #1276, Version 3, Updated January 3, 2010

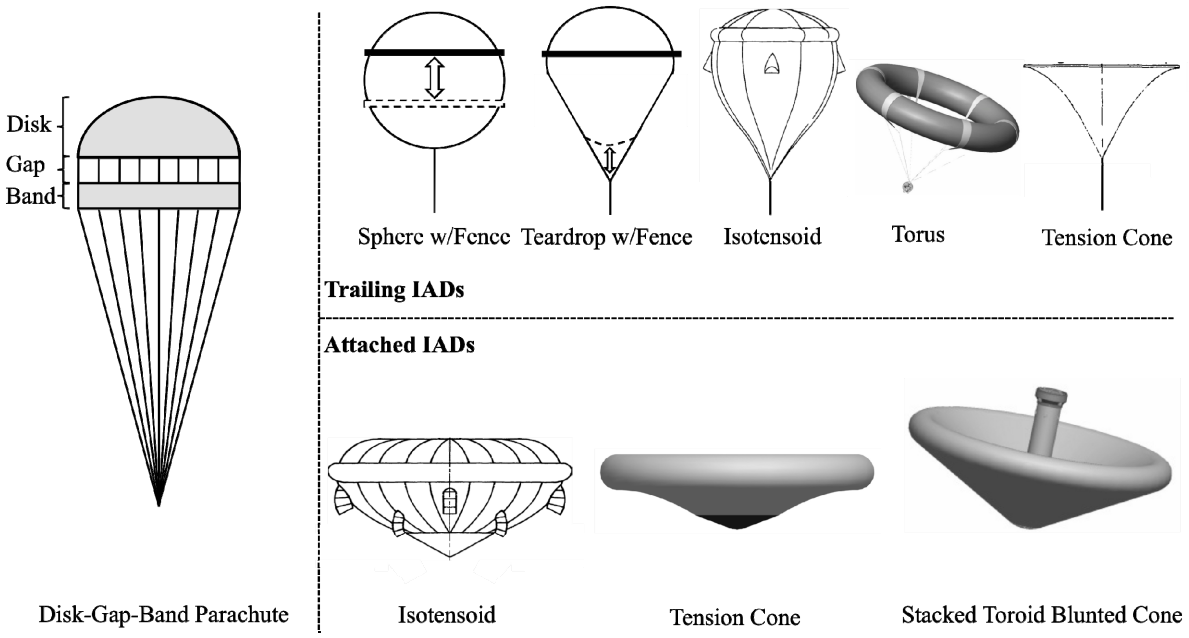


**Figure 1. Examples of feasible trailing and attached IAD configurations and a Disk-Gap-Band parachute.**

## 2. TESTED CONFIGURATIONS

Dozens of trailing and attached IAD geometries have been tested in wind tunnels and even more conceived in system studies. Configurations with documented aerodynamic or aerothermodynamic test data available in the literature [11]-[60] are shown notionally in Figure 1. Also shown is a notional DGB parachute similar to those used on many planetary probe missions.

Technical discussions in this survey concentrate on the following three IAD sub-configurations: the isotensoid, the tension cone, and the stacked-toroid blunted cone. Many other configurations have been studied in the past, including some asymmetric configurations intended to fly with positive hypersonic L/D [61]-[63]. However, technology investments in the past decade have revealed the aforementioned configurations as those with the highest probability of application to a future planetary probe mission. Figure 2 illustrates the scope of successful flight test experience with SIADS and HIADs as a function of deployment dynamic pressure and Mach number since their conception in the 1960's. For reference, a deployment Mach number of 2.2 and dynamic pressure of 750 $N/m^2$ is presently planned for the Mars Science Laboratory (MSL) DGB parachute, setting a new deployment bound for this system [64].

The following sections are meant to serve as an aggregation of available data and major technical findings for these IAD configurations. Quantitative data is presented directly while qualitative data is indexed from the literature. In some cases it is more appropriate to segregate discussions by IAD configuration (e.g. aerodynamics), while in others it is appropriate to divide discussions by whether or not the IAD is trailing or attached to an aeroshell (e.g. stability).

## 3. DEVELOPMENT HISTORY

American IAD development began in the 1960's when NASA Langley Research Center (LaRC) proposed using inflatable vehicles for manned atmospheric reentry [65]. In the nearly fifty years since IAD development began, dozens of different IAD configurations have been analyzed and tested at a suite of flight conditions for numerous military and exploration-related applications. The Air Force and NASA led early IAD testing in separate efforts, with much of the test article construction and data analysis performed for both entities by the Goodyear Aerospace Corporation (GAC) and other contractors between 1961 and 1974 [11]-[60]. A summary timeline of IAD development history from 1960 to the present day is shown in Figure 3.

IADs reached their peak technology readiness in the mid-seventies during the mission planning phases of the Viking, Pioneer Venus, and Galileo missions. These planetary missions were the first to require deployable decelerators during atmospheric descent. Also in the later stages of technology development at the time was the DGB parachute. Although it was shown to be a capable decelerator, the DGB parachute exhibited inflation issues and area oscillations above Mach 2. The IAD showed potential during wind tunnel tests as a supersonic decelerator capable of operating beyond the DGB performance thresholds. Mission studies revealed that Viking did not require a parachute deployment above the Mach 2 threshold and that the Pioneer Venus and Galileo missions were possible with Earth-based parachute technology [1]. Without a need for decelerator operation outside of the DGB parachute's performance envelope, work to further mature the IAD ceased in the mid-1970s, leaving many IAD design concerns unaddressed.

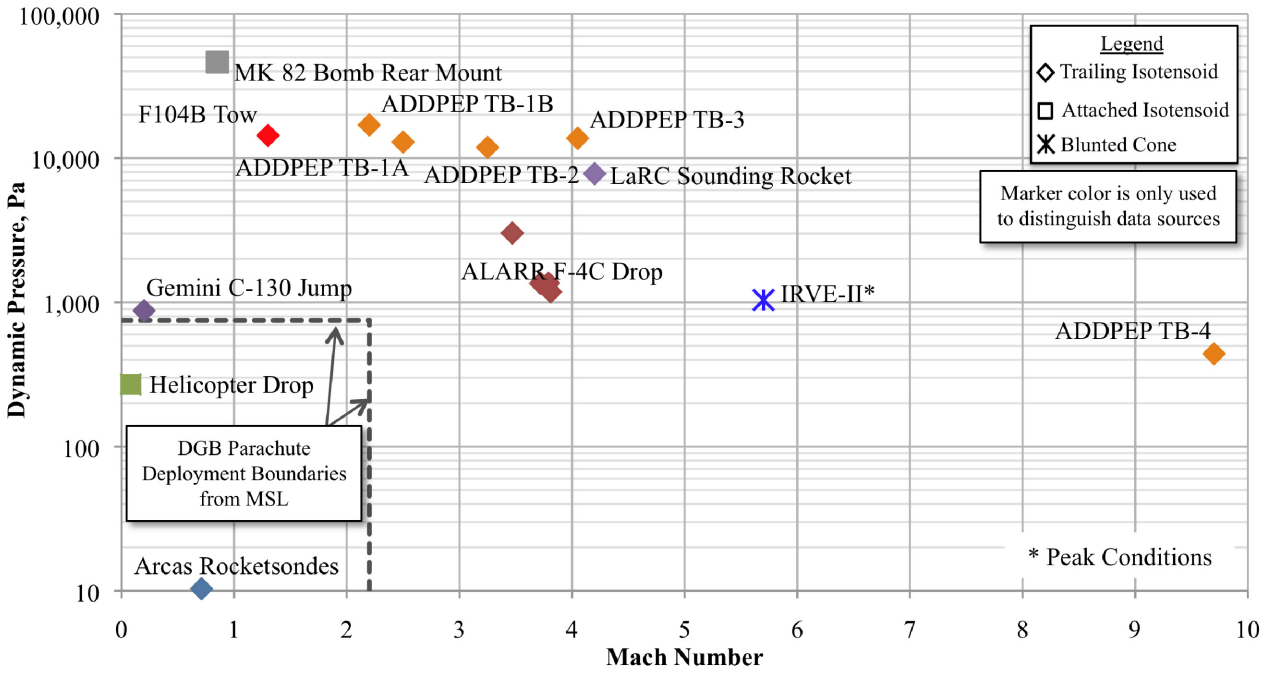


**Figure 2. Successful IAD flight test deployment conditions (*exo-atmospheric inflation, peak conditions shown).**

Over twenty years passed before the IAD concept was revisited by Pioneer Aerospace [66] in 1995. IAD development was minimal during this period as resources were refocused to other projects. GAC, the main proprietor of IAD technology during the 1960's, was absorbed by the Loral Systems Group in 1987, and was again sold to Lockheed-Martin in 1996 [67]. At this time it is unknown if the original flight articles tested by GAC or the original wind tunnel and flight test data records were preserved.

Interest in the IAD has renewed in recent years from numerous atmospheric entry trajectory analyses at Earth, Mars, Titan, and Neptune calling for deployable decelerator operations outside of the DGB performance envelope [1]-[10]. The results can be divided into those that reveal the IAD as a mission-enabling technology or those that reveal the IAD as a technology capable of adding substantial performance increases compared to existing decelerator technology. The collective conclusion of this work is clear: many robotic and human planetary exploration missions will remain beyond our reach if engineers continue to rely on 1960's-era deployable decelerator technology.

Although worldwide IAD development in the past decade has led to substantial technology maturation, present-day IAD technology readiness remains lower than it was prior to the Viking launch. Numerous distinct technology development efforts have been executed over the last decade by the Air Force [68], the Defense Advanced Research Projects Agency (DARPA) [69], Lockheed Martin [70], the European Space Agency (ESA) [71], and NASA [72]-[76]. Current IAD technology investments are tunneled through the Fundamental Aeronautics Hypersonics Project and Advanced Decelerator Technology (ADT) program, and the recent wind tunnel tests at NASA LaRC were funded through the Program to Advance Inflatable Decelerators for Atmospheric Entry (PAIDAE). These investments include the successful 2009 flight test of the Inflatable Reentry Vehicle Experiment (IRVE), a stacked-toroid blunted cone HIAD geometry. Incremental and sporadic technology advancements will certainly continue along the current programmatic trajectory, but a coordinated technology development effort is needed at the agency-level [77] before the IAD can be fully realized as a mission-enabling Entry, Descent, and Landing (EDL) technology.

## 4. AERODYNAMICS

Deployable decelerators have three primary functions for use in planetary entry vehicles: system deployment, stability, and deceleration. IADs can be used for all of these functions, but the latter two are the focus of this discussion. Aerodynamic force measurements exist for all of the configurations in Figure 2, but the configurations with the most complete data sets are the trailing isotensoid, attached isotensoid, attached tension cone, and attached blunted cone. Blunted cone (sphere-cone) data for various cone half-angles is widely available for various cone half-angles, and thus is not discussed here. This section discusses the aerodynamic performance at zero angle-of-attack of the first three configurations based on their measured drag performance taken from the literature. The data shown includes rigid and flexible test articles. Aerodynamic data for these configurations at a wide range of angles-of-attack is available in the literature. All drag coefficients are referenced to the projected area for all decelerators. This projected area includes the burble fence for isotensoid configurations.

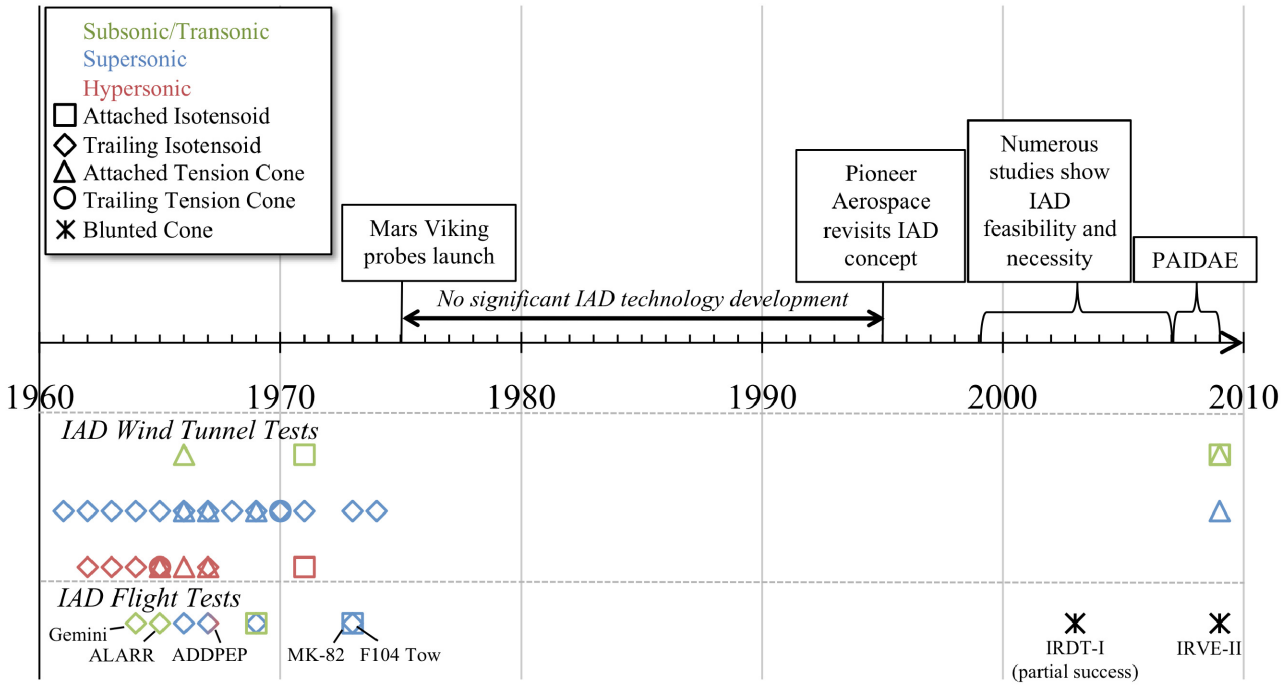


**Figure 3. History of IAD technology development efforts.**

## *Trailing Isotensoid*

Figure 4 shows all documented trailing isotensoid wind tunnel and free-flight aerodynamic test zero degree angle of attack drag data. Most isotensoid IADs are outfitted with a mechanism designed to induce uniform flow separation known in the literature as a burble fence. Data markers with an edge border indicated the presence of a burble fence. The colors of the data points indicate the non-dimensional towline length, $l_t/D_f$, where $l_t$ is the distance from the IAD to the base of the leading body and $D_f$ is the outer diameter of the leading body. Marker shapes indicate the geometry of the leading body as slender or blunt. Cone half-angles among tested trailing isotensoid configurations vary from 30º to 40º. The data does show a general drag trend: drag coefficient increases until approximately Mach 1.5, decreases until approximately Mach 5, then levels off in the hypersonic regime. Additionally, trailing isotensoid drag performance is a strong function of non-dimensional towline length.

Computing the optimum towline length to maximize decelerator performance requires a complete understanding of the leading body wake flow field. During early trailing isotensoid development, Nerem [78] developed an approximate method to compute flow properties of the inviscid wake behind a blunt body moving at hypersonic speeds. Recognizing the superficial treatment of wakes in the transonic and supersonic flow regime, Jaremenko [79]-[80] summarized theoretical and experimental attempts to predict wake qualities throughout the various wake flow regimes: near, laminar, transition, turbulent, and growth.

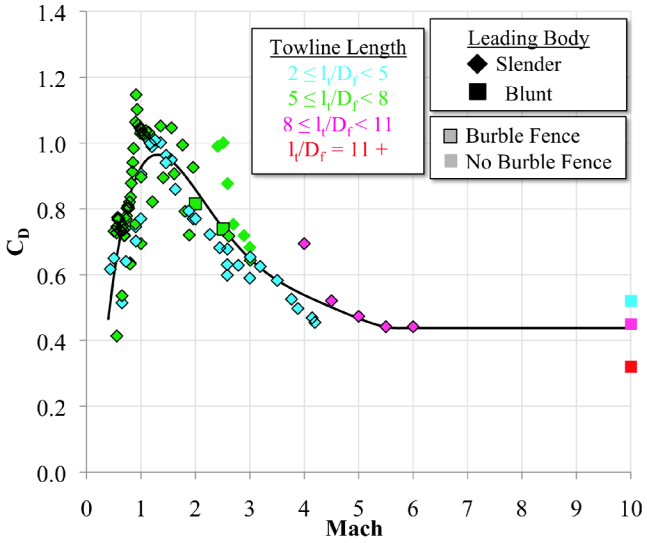


**Figure 4. Trailing isotensoid drag performance data.**

One accepted conclusion from this work is that IADs operating in the wake of a leading body must operate in disturbed flow at a local Mach number lower than freestream, as shown in Figure 5. This momentum deficit weakens the IAD bow shock and leads to lower surface pressures than attached IAD configurations. As such, trailing IAD configurations tend to experience less drag than their attached counterparts. The trailing isotensoid database in Figure 4 uses several data sets to verify this hypothesis. More recent analytic wake flow characterizations focus mainly on the hypersonic flow regime [81]-[82]. Without a

rigorous analytical treatment of wake flow throughout the entire flight envelope, predicting IAD drag performance in the wake of a leading body remains an empirical effort.

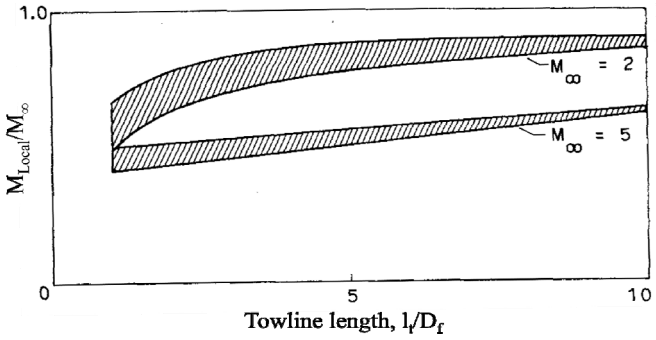


**Figure 5. Mach number variation in near wakes [80].**

## *Attached Isotensoid*

Technology maturation transitioned from trailing configurations to attached configurations in the late 1960's in large part due to the improved aerodynamic performance and potential mass savings. Recognizing the unmet need for a viable supersonic and hypersonic decelerator, NASA LaRC initiated an extensive research program to mature an attached isotensoid IAD configuration [40] in this timeframe. Wind tunnel and free-flight test data for the attached isotensoid is aggregated in Figure 6. Several data sources agree on the drag performance in the Mach 2 to Mach 5 regime, but subsonic and transonic aerodynamic data is sparse. A December 2009 test conducted in the Transonic Dynamics Tunnel (TDT) at NASA LaRC under the Advanced Decelerator Technology (ADT) program will help to populate this flow regime. Hypersonic drag data has not been measured but should be similar to that in the supersonic regime.

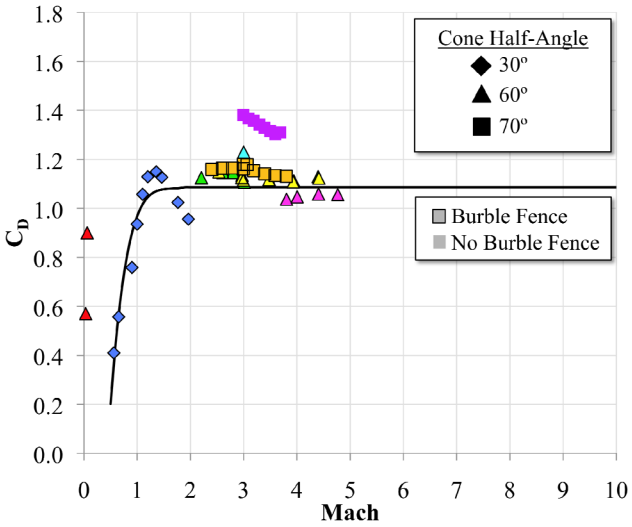


**Figure 6. Attached isotensoid drag performance data.**

Only one data set is known where the test article did not employ a burble fence to induce uniform flow separation [60]. The data shows that, although required at subsonic speeds, the burble fence is an aerodynamically inefficient device at supersonic speeds. That is, the burble fence increases the IAD projected diameter, but does not increase the drag performance by the same proportion resulting in a net reduction in drag coefficient at supersonic or hypersonic speeds. A burble fence height equal to 5% of the isotensoid equatorial diameter is an accepted sizing rule to reliably induce uniform flow separation at subsonic speeds while minimizing aerodynamic inefficiency.

## *Attached Tension Cone*

During the period of heavy trailing isotensoid testing, Anderson [83] suggested a new IAD geometry called the tension shell. This shell of revolution is designed to have only tensile stresses under axisymmetric aerodynamic loading. The tension cone refers to the entire IAD configuration consisting of the tension shell and the rigid or pressurized compression ring required to hold the tension shell shape. Aerodynamic drag performance data from known wind tunnel tests is shown in Figure 7.

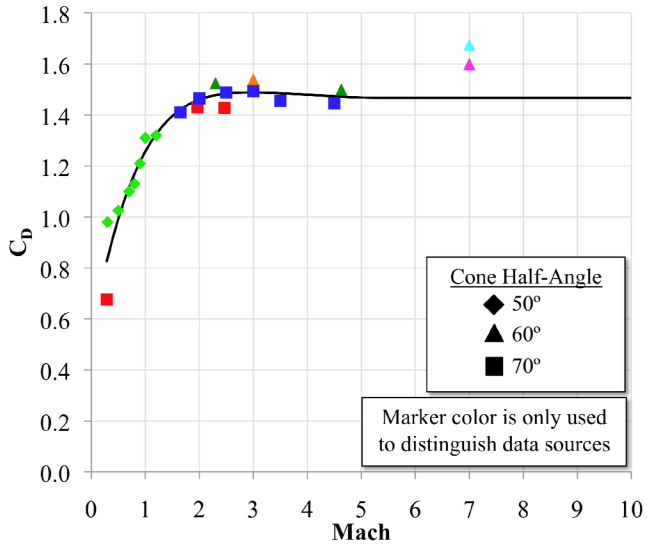


**Figure 7. Attached tension cone drag performance data.**

Tension cone wind tunnel tests and computational analyses reveal this configuration as an aerodynamically viable SIAD. The tension cone's concave surface geometry may prevent the extension of this decelerator to the hypersonic flow regime due to concerns of embedded shocks and the associated aerothermodynamic difficulties. Additionally, Modified Newtonian theory is a poor predictor of the hypersonic surface pressure distribution over the concave tension shell [27], thus necessitating the use of integral-relation methods [84] or numerical Computational Fluid Dynamics (CFD) solutions to compute surface pressures.

Clark [85] independently verified many of the 1960's-era aerodynamic conclusions in supersonic wind tunnel tests conducted in 2008 at the NASA Glenn 10'x10' (fully inflated and semi-rigid configurations) and the NASA LaRC

Unitary Plan (rigid configuration) wind tunnels. These tests investigated the aerodynamic characteristics of the tension cone at various supersonic Mach numbers and angles of attack. Embedded shocks were not observed.

Earlier test results showed that the isotensoid IAD had a tendency to align itself with the direction of the flow far ahead of the body while operating at angle of attack [49]. Clark did not observe these phenomena with the tension cone: the degree of non-alignment with the freestream never exceeded two degrees. This behavior is likely due to the stiffness of the torus and the nature of the tension shell to maintain tension in the meridional direction. Such behavior is desirable for tension cone geometries because alignment with the freestream could initiate torus buckling and/or tension shell wrinkling [85].

### *Drag Performance Comparison*

Figure 8 shows the best estimate zero angle of attack drag trends with Mach number based on numerous data sources. Shown are the attached configurations of the tension cone and isotensoid, the trailing isotensoid, and the DGB parachute. Exploratory investigation of trailing tension cone performance has taken place [24][50], but extensive performance testing was never initiated for this geometry. In the supersonic and hypersonic regimes, the attached tension cone offers considerable benefit. In contrast, the DGB parachute has superior subsonic drag performance over all IADs. DGB drag data is limited to Mach 2.5 and lower due to known area oscillation issues and inflation difficulties encountered at Mach numbers higher than this threshold [86]. The transonic drag bucket at Mach 1 for the DGB is behavior absent in all IAD test data. Wind tunnel data for the three IAD configurations generally covers the supersonic regime well but is either extrapolated or based on sparse data in the hypersonic regime.

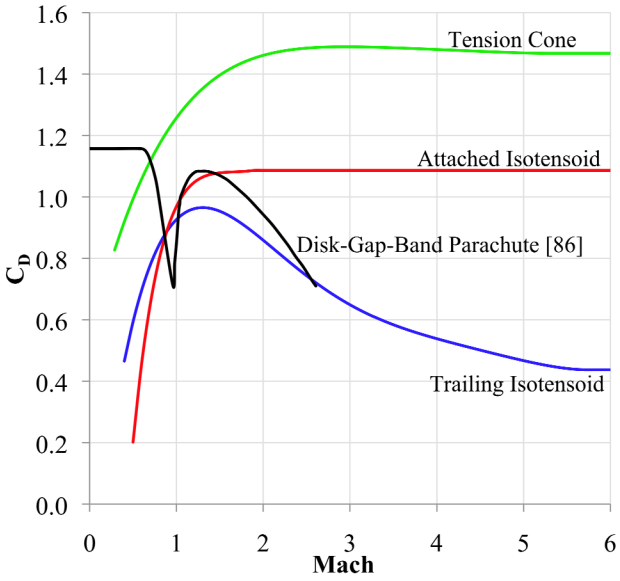


**Figure 8. IAD and DGB parachute drag comparison.**

## 5. AERODYNAMIC STABILITY

A midterm survey of IAD development in 1966 [87] emphasized that there existed no documented, quantitative, experimental dynamic-stability data for the trailing and attached configurations of the isotensoid and tension cone. Dynamic stability data collected from wind tunnel tests and flight tests prior to 1970 was limited to visual observation. It is common in the literature to see vague language like "excellent, good, fair, poor" as the sole indication as the to the degree of IAD stability. Such data can only be used for creating ordinal rankings of IAD alternatives. Isotensoid and tension cone static stability is discussed below. Attached blunted cone static stability is understood and data is widely available in the literature [88]. Ballistic range testing at Eglin Air Force Base for the IRVE geometry quantified dynamic stability for blunt cone geometries [89].

### *Trailing Isotensoid*

At present only qualitative stability observations exist for trailing IADs. Although towed isotensoid static stability is not a strong function of Mach number, the effective IAD frontal angle needs to be relatively small in order to assure stability of the two-body configuration. That is, a blunt body trailing another blunt body is less stable than a slender body trailing a blunt body [40]. The observed positive correlation between leading body bluntness and wake flow unsteadiness may explain this trend, but the later parameter is difficult to quantify. Any future test program for trailing IAD configurations must include analyses to quantify the multi-mode motion.

### *Attached Isotensoid*

Several attached isotensoid tests in the Viking-era demonstrate statically stable configurations of the attached isotensoid IAD [45][48][49]. Bohon and Sawyer [60] discourage the addition of a burble fence for supersonic operations but emphasize the necessity of a burble fence for stable subsonic operations. A subsonic payload extraction study in 1971 showed violent oscillations below Mach 0.5 for attached isotensoid configurations without a burble fence [90]. Dynamic stability (pitch damping coefficient) of the attached isotensoid has not been measured.

### *Attached Tension Cone*

The tension cone is statically stable in supersonic and hypersonic flight as long as the flow remains attached to the tension shell surface [85]. Clark arrived at this conclusion in a survey of the early tension cone wind tunnel tests and confirmed the result in the series of recent PAIDAE wind tunnel tests. Dynamic stability of the tension cone has not been measured.

## 6. AEROTHERMODYNAMIC LOADING

Some proposed missions require the use of IADs in high heating environments. While SIADs generally sustain low to moderate levels of heating, depending on mission design considerations, HIADs could experience high levels of heating. Therefore, the heating environment must be accurately characterized and the IAD must be designed to sustain such an environment. Both computational and experimental efforts are required to compute the heating environment. Accurate simulation of the aerothermal environment of an IAD system is made difficult by large-scale geometries and the possibility of unsteady deformations. Subsequent computation of material thermal response requires temperature-dependent material properties, and this data is still not available for many materials of interest. Furthermore, it is difficult to validate computational results for large IADs using current experimental capabilities.

Trajectory analyses typically show that HIADs must be significantly larger than conventional rigid aeroshells in order to give the desired system benefits. As such, a complete aerothermodynamic analysis should also consider the potential for elevated radiative heating. The convective heating experienced by the large and flexible IAD system may be lower than for the rigid aeroshell alone, but the observed aerothermal environment is highly dependent on the shape and configuration used. The previous computational and experimental work for the IAD geometries of interest is summarized here.

### *Trailing Configurations*

In 1962, Kayser [14] performed wind tunnel testing to measure surface heat transfer rates for a trailing isotensoid IAD at Mach 10. These tests demonstrated that the heating was as much as twice as high when the model was tested without a leading body, indicating that generally the trailing IADs experience lower heating compared to attached ones at the expense of lower drag. In 1965, Nebiker [23] performed thermodynamic analysis for a trailing isotensoid IAD configuration. He assumed that the IAD flowfield is not affected by the leading body. In phase II of the same program, Bloetscher [33] improved the analysis by using methods to characterize the wake flow behind the leading body and then compared his analysis with flight data. Figure 9 shows the comparison as a function of time of flight. Relevant to this discussion are the relative values of the two pairs of solid black lines and the corresponding thermocouple data (one pair for atmospheric exit phase, one pair for atmospheric entry phase). The comparison showed that the developed analytical methods yielded a moderate degree of accuracy in establishing the wake aerothermodynamic environment and material temperature response.

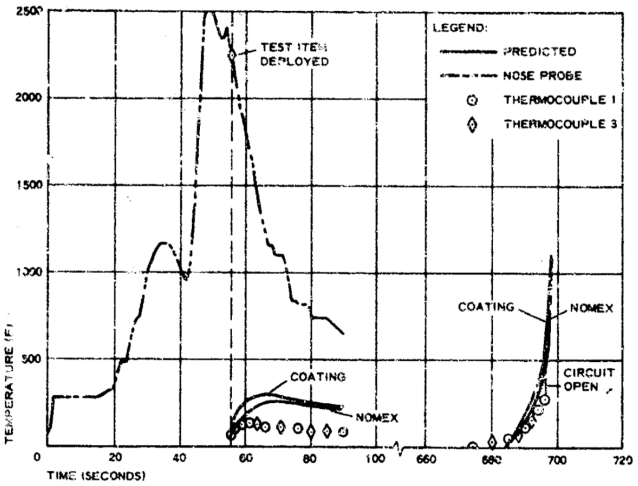


**Figure 9. Predicted and measured temperatures of a trailing isotensoid flight test at Mach 9.7 (article TB-4 of ADDPEP) [33].**

The advent of CFD provided engineers with the opportunity to develop a more accurate analytical characterization of the IAD heating environment. In 2001, Hornung [91] performed a series of time-accurate inviscid CFD solutions for vehicles with elliptical and toroidal towed IADs. Gnoffo and Anderson studied toroidal and spherical trailing IADs using the LAURA algorithm including viscous and high temperature effects [92][93]. In 2006, Gnoffo et al. examined two challenging aspects of aerothermal simulation of trailing IADs: the simulation of a complete system including tethers, and the detection of the onset of the unsteady flow interactions [94].

Experimental data are required to validate the computational characterization of the IAD heating environment. Rasheed et al. performed heating tests on toroidal IADs in the Graduate Aeronautical Laboratories, California Institute of Technology (GALCIT) T5 Hypervelocity Shock Tunnel [95]. In 2004 McIntyre et al. performed a test similar to GALCIT test but with higher freestream enthalpy to capture the effects of dissociation and ionization [96]. In conclusion, the trailing IADs will generally see lower heating rates; however they can experience significant flow unsteadiness due to wake and shock interactions between the IAD and the leading body.

### *Attached Configurations*

In 1971, Faurote and Burgess [56] attempted to characterize the aerothermal environment for an attached isotensoid IAD. Convective heat rate relations were developed for both laminar and turbulent conditions by using boundary layer equations based on the local similarity concept. In the same year, Creel [46] performed wind tunnel testing to investigate the aerodynamic heating of attached isotensoid IAD configurations at Mach 8. Heat-transfer coefficients were obtained using a fusible-temperature-indicator technique that employed temperature sensitive materials that melted into a clear liquid at a certain temperature. The results

showed that heating on the ram-air inlets and burble fence were approximately five times larger than the smooth IAD body. The localized heating at ram-air inlets showed that exoatmospheric inflation might be preferred to ram-air inflation for HIADs. Furthermore, it was observed that areas of local flow separation in the vicinity of the aeroshell-IAD attachment or burble fence attachment experienced lower heating rates.

The heating profiles for attached tension cone configurations were examined with wind tunnel testing at Mach 7 [24], Mach 8 [32], and Mach 20 [27]. A common observation was the presence of an attached shock near the back of the tension shell. This attached shock was mainly due to the concavity of the tension shell. It was also observed that the heating rates increased considerably in the post-shock region. These results suggest difficulties with using a tension cone configuration in high-Mach hypersonic flight. Gnoffo and Anderson performed CFD studies for a spherical attached IAD and observed neither shock interactions nor flow unsteadiness [92][93]. In general, the unsteady flow observed with trailing IADs can be avoided using attached IADs, however they will experience higher heating rates and potentially shock interactions and attached shocks for certain geometries.

## 7. Structural Analysis and Testing

A difficulty in optimized IAD design involves creating a shape that is loaded in tension in both principle directions simultaneously. Due to the membrane properties of IAD materials, wrinkling or buckling will occur if tension loads vanish in one direction. Wrinkling introduces unpredictable behavior into the aerodynamic surface that can create localized stress concentrations, induce flutter and other undesirable aeroelastic effects, and contribute to localized heating. Thus, most structural design and analysis of IADs involves using linear theory to determine the shapes and stresses necessary to maintain biaxial tension against a known aerodynamic load.

Limited static structural testing of IADs has been performed in bench tests and vacuum spheres. However, the fact that the aerodynamically deformed shape cannot be achieved outside of a wind tunnel raises questions as to the utility of these tests. Additionally, it is not clear how to obtain a relevant in-situ stress measurement on a curved membrane surface due to the inherent stiffness in the measurement device itself. Static structural tests will become more important as IAD structures become larger and are unable to be properly tested in a wind tunnel.

### *Isotensoid*

In 1964, Houtz [97] proposed a decelerator design with two primary structural elements – uniaxially-loaded meridional cords surrounding a biaxially-stressed envelope. Isotensoid theory provides for stresses that are equal in both principle directions of the envelope and constant across the entire surface. Similarly, tensile loads in the meridional cords are constant along their entire length. These properties are advantageous to overcome flutter and stability problems inherent in parachutes. The isotensoid properties hold throughout the decelerator except at the ram-air inlets or in the presence of a burble fence, which creates a discontinuity in stresses between the front and rear surfaces. Additionally, differences in the elastic properties between the envelope fabric and the meridional cords cause the envelope to lobe in between each meridian, slightly changing the envelope stresses. Barton [39] develops an analytical expression to calculate the stresses of a lobed isotensoid surface based on the design stress, internal pressure, number of gores, and material bias.

Static structural experimentation of the GAC 1.5-m isotensoid models consisted of shape verification, inflation loads estimation, and material strength testing. To verify the envelope's shape in the absence of aerodynamic loading, two lab fixtures were constructed in the form of a foundry sand mold [39] and a conical cage [52] to properly position the front surface and locate points on the rear surface. Structural parameters such as static meridional loading and envelope burst pressure were obtained by fastening the decelerator's rear surface into a conical test fixture [57] and splicing load cells into the meridional cords. These static tests helped illustrate some of the limitations of using linear theory, which primarily deal with lower-than-predicted measured loads due to unaccounted for elasticity in the meridional cords.

### *Tension Cone*

In 1965, Anderson introduced an optimal decelerator design in which a surface of revolution (tension shell) is shaped to exhibit only tensile stresses in both principle directions and transfer only compressive loads to a hoop-shaped support member [83]. This concept was later expanded to incorporate an inflated torus as the support member, allowing a fully inflatable system. Sizing of the torus involves quantifying the compressive loads on the ring and using linear membrane theory to determine the required internal pressure, minor diameter, and material properties to resist wrinkling at the peak compressive load [98]. However, advanced fabrication techniques may have potential to decrease inflation pressure, and thus torus mass, beyond that predicted by linear theory [99].

Fabrication limitations may require both the torus and tension shell to be constructed of more than one piece of fabric. The non-circular cross section of the resulting shape creates a significantly different stress state in both parts than predicted by linear theory. Static structural tests have not been performed on either a continuous or faceted tension cone design to obtain shape verification and structural parameters.

### *Stacked Toroid*

An inflatable conical forebody can be created by stacking a series of concentric toroidal bladders of increasing diameter and wrapping them in a thermal protection layer to create a smooth surface [73]. The shape of a stacked toroid IAD is not a direct function of the aerodynamic pressure distribution, but the aerodynamics do affect the toroid pressures and thus the system mass. Toroid inflation pressures can be estimated given an aerodynamic load by calculating the pressure required to resist compressive buckling of each torus due to the applied forebody load [100]. However, analytical expressions to calculate the biaxial stress and mass of a system do not exist, making parametric analysis of the stacked toroid and a direct mass comparison against the other shapes difficult. This construction method was successfully demonstrated by the IRVE flight test [101].

### *Aeroelastic Analysis*

Before the advent of high-speed and Massively Parallel Processing (MPP), it was necessary to develop analytical relationships to predict aeroelastic behavior. In the 1960's, both Anderson [83] and Houtz [97] developed the tension shell and isotensoid shapes, respectively, by using analytical structural theories and applying a distributed load in the form of an arbitrary aerodynamic pressure profile. In the 1980's, Park [102] developed an analytical approach to study the drag of a trailing ballute as a function of its internal pressure. These methods of combining aerodynamic and structural theory to create aeroelastic response are elegant, but impose several simplifying assumptions that limit their usefulness to first-order approximations.

Scientific computing has enabled Finite Element Analysis (FEA) of deformed structures and CFD analysis of flowfields around rigid bodies. Fluid-Structure Interaction (FSI) frameworks couple together FEA and CFD to simultaneously investigate how an aero-structure changes to a given flowfield and how the flowfield subsequently changes around the deformed structure. Development of FSI capabilities emerged in the late 1990's with the development of the MONSTR code by Mosseev [103]. In the 2000's, Rohrschneider [6] coupled two independent FEA and CFD codes together: commercial FEA code (LS-DYNA) and a Cartesian-based Euler solver (NASCART-GT) to achieve a good qualitative match to experimental data as seen in Figure 10.

NASA grants from the Fundamental Aeronautics Program Hypersonics Project have allowed the recent development of two monolithic FSI codes. Candler and Pantano [104] created a capability to analyze flowfields with strong shocks around a membrane structure. Gilmanov [105] created a framework that solves the Navier-Stokes equations around a deformable Eulerian solid.

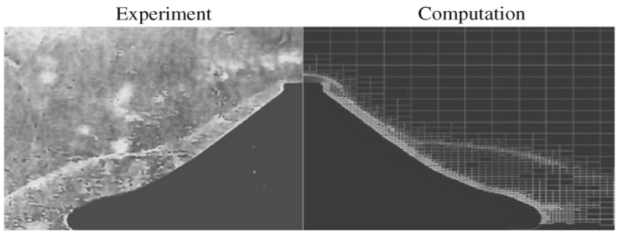


**Figure 10. Comparison of computational and experimental aeroelastic shape [6].**

Current issues with computational FSI analyses include long run times and lack of quantitative validation data. Most FSI validation efforts rely on qualitative comparison against images acquired during experimentation. In-situ measurement of displacements and stresses on membrane-like structures is difficult given that instrumentation, such as a strain gauge, can significantly change the local material properties. Photogrammetric methods show promise in acquiring quantitative aeroelastic validation data, but have only recently been used in wind tunnel experiments involving textile-based decelerators.

### *Scaling Issues*

A primary concern of IADs is the aeroelastic consequences of scaling these devices to the size required for flight, which might be orders of magnitude larger than what can be tested in wind tunnels. Prevention of wrinkling and flutter conditions becomes more difficult as flow becomes turbulent over the large IAD surface. Additionally, membrane wrinkling and buckling loads do not scale linearly with size [106]. Nonlinear finite element analysis will be one method of mitigating this risk, but it will require some static structural data with which to be anchored. Obtaining such data for these devices is a challenge in itself for aforementioned reasons.

Recognizing the lack of historical precedence for designing full-scale inflatable structures, NASA LaRC constructed and successfully flight-tested an 11 m (36 ft) diameter subsonic attached isotensoid in 1969, shown below in Figure 11. Ram-air inlets on the surface of the aeroshell provided initial inflation, with additional inlets located on the envelope assisting inflation as soon as they were exposed to the freestream [48]. Recent studies have called for SIADs up to 50 m (164 ft) in diameter [9]. There is currently no cogent and funded technology maturation plan in place to meet this challenge for future EDL systems.

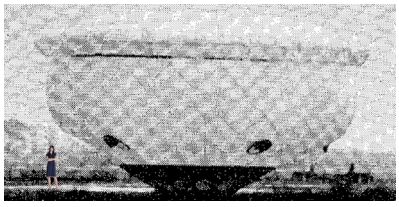

**Figure 11. Subsonic flight test article of large-scale attached IAD with human added for scale [48].**

### *Mass Estimation*

Parametric mass estimation techniques exist for the supersonic configurations of the tension cone and isotensoid IADs [107][8]. These methods generally involve computing the required material acreage and then assuming uniform material areal density to determine envelope mass. For non ram-air inflated articles like the tension cone and some configurations of the isotensoid, an inflation system including required inflation gas must also be sized. Often extra mass is allocated for porosity-reducing coatings. A caveat of these first-principles methods is that full-scale flight articles constructed for the flight regimes for which the IAD is intended have never been constructed. As with any new technology, obtaining highly accurate mass models for these IAD geometries will require a bottom-up component-based method. Brown has performed this type of component-based mass estimation for a SIAD tension cone configuration [108].

Despite their limitations, these first principles mass models are useful for comparative analyses of different configurations and sensitivity analyses. A comparison of SIAD mass for the trailing isotensoid, attached isotensoid, and tension cone is provided below in Figure 12 for various design dynamic pressures. The deployment dynamic pressure is usually the peak dynamic pressure for SIADS, so this value is taken as the design limit. The shown dynamic pressures are selected to capture deployment conditions relevant for Mars entry and flight-testing at Earth. The mass estimation methods for the isotensoid and tension cone are taken from work by Anderson [107] and Clark [85], respectively. The material is assumed to be Nomex coated with Viton (minimum gauge areal density of 0.078 kg/m$^2$), and all other inputs are consistent with [107] and [85] with the exception of the isotensoid drag coefficients. Drag data is taken from the wind tunnel data curve fits provided earlier in this paper assuming IAD deployment at Mach 5. Parametric mass estimation methods for the stacked toroid remain as an area of future work.

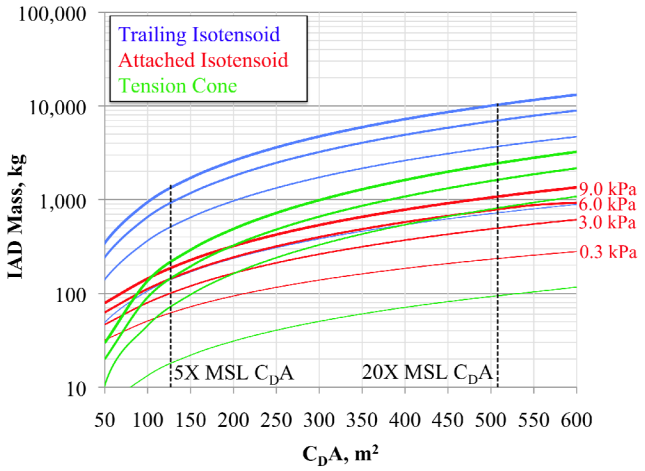


**Figure 12. SIAD mass as a function of drag area and deployment dynamic pressure.**

The SIAD mass estimates show that the trailing configuration is always heavier than the attached configuration of the isotensoid for a given dynamic pressure. This is attributed to the extra mass of the towline and the substantially lower drag coefficient (57%) of the trailing configuration. The towline is sized to support the entire drag force on the trailing IAD, so the mass of this component is highly sensitive to the operating dynamic pressure. The tension cone has lower mass than the attached isotensoid for low deployment dynamic pressures, as may be the case at Mars. However, modest increases in deployment dynamic pressure may reveal the attached isotensoid as more favorable. For instance, the attached isotensoid has a lower mass than the tension cone for a deployment dynamic pressure of 3.0 kPa for drag areas less than 200 m$^2$. Masses of fabricated full-scale articles will likely diverge from these first-order trends due to complex seaming and joining schemes.

Mass models for HIAD configurations need to accommodate the additional complexity of aerothermodynamic loading by accounting for thermally resistant fabrics. These articles may be constructed of non-uniform multi-layer material layups, as was the case for IRVE. Such design conditions make parametric mass estimation of hypersonic IADs challenging. Point-design mass estimates for some HIAD configurations have been made, but these generally do not account for material thermal response or rely on material acreage computations for a specific drag area and deployment condition [7][75].

## 8. Atmospheric Inflation

IADs are inflated with an internal gas source, ram-air, or a combination of both. In ram-air inflation, the IAD is outfitted with inlets that inflate the IAD when exposed to the high dynamic pressure freestream. Inflation via an internal gas source requires the EDL system to carry an internal gas generator or tanks of pressurized gas. The internal gas source inflation scheme is a requirement for tension cone IADs due to high torus pressure requirements and exo-atmospherically inflated IADs due to lack of dynamic pressure. The IRVE-II flight test in 2009 demonstrated the first successful exo-atmospheric inflation of an IAD. Among atmospheric inflation methods, trailing IADs have all been ram-air inflated and generally inflate without issue. Attached IAD inflation schemes are discussed in the sections below.

### *Attached Isotensoid*

In early wind tunnel tests, initial canopy deployment was assisted by a water-alcohol mixture that would vaporize at low pressure and provide enough internal envelope pressure to expose the inlets to the high dynamic pressure flow. This effective inflation process and was used for several attached isotensoid wind tunnel tests [38][42][51]. Concern over the large amount of liquid that would be required for a full-scale decelerator system and the associated mass penalty led to

the development and testing of mechanically deployed inlets. This method was also quite successful in wind tunnel tests [47][52][55][60]. Ram-air inflation virtually eliminates deployment load overshoot commonly associated with parachutes. The inlets provide controlled flow into the canopy, so the flow rate decreases rapidly as the internal pressure nears twice the freestream dynamic pressure [51].

### *Attached Tension Cone*

Most early tests of the tension cone geometry were for rigid aeroshell applications. Kyser [36] was the first to investigate the use of an inflatable torus as the aft tension cone compression ring. The study focused on the load-carrying ability and failure modes of the inflated tension cone before and after deployment. Underwater deployment tests were conducted to develop deployment techniques for later aerodynamic testing at supersonic speeds.

In 2008, tension cone wind tunnel tests for the PAIDAE program included a fully inflated configuration [85]. Figure 13 shows how the Kevlar article was inflated with tubes on the back of the torus connected to the sting hardware. An additional configuration (not shown) used anti-torque panels on the rear of the tension cone to prevent the flexible torus from rolling forward. Expedient deployment and inflation was observed. The configuration outfitted with anti-torque panels required dramatically less inflation pressure for complete deployment.

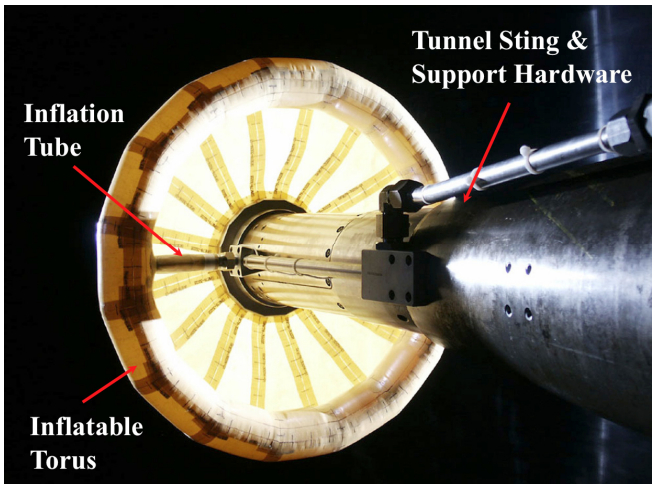


**Figure 13. Aft view of the inflatable tension cone model installed in the test section [85].**

## 9. MATERIALS

Exo-atmospheric inflation and high heat loads during entry require that hypersonic IAD materials have good heat resistance, strength retention under thermal loading, chemical stability in an oxidizing environment, and very low porosity. High material strength may not be necessary for hypersonic applications as most of the deceleration is likely to occur at low dynamic pressures. The high aerodynamic loads anticipated for supersonic IADs, however, require that materials have high strength, high elastic moduli, and moderate thermal resistance against turbulent heating conditions.

### *Historical Materials*

In the 1960's, state of the art materials consisted of woven fabrics of synthetic fibers, such as Nomex, nylon, and Dacron [87]. These fabrics exhibited the best strength retention under prolonged thermal (up to 400°F) and structural load, with Nomex as the best of the group. Additionally, filament materials (fabrics of woven metal or ceramic strands) were tested and showed a resistance to temperatures exceeding 1000°F. Filament materials were not seriously considered due to their prohibitively high cost. Nomex was ultimately selected to construct the GAC isotensoid models.

A multifilament stainless steel fabric was used in an alternate, lifting IAD concept designed to re-enter a single human passenger from an Earth-orbiting space station [61]. This study concluded that metal filaments would have to be drawn to very small diameters to reduce bending rigidity enough for sufficient flexibility for packing and crease recovery when inflated. A custom-built spot welder was required to join metal fabric segments to create the decelerator.

Elastomeric coatings were tested as a means of reducing fabric porosity and adding more thermal protection to the base fabric [87]. Urethane- and silicon-based coatings showed promise in reducing porosity and showed limited applicability as thermal protection. One study recommended the use of ablatives on the surface of an IAD to increase its thermal resistance, but acknowledged that such a coating would be quite sophisticated [109]-[110]. Extensive information regarding charring and gas retention of several silicon rubber elastomers at elevated temperatures is given in Ref [61].

### *Modern Materials*

In 2009, a series of high-temperature tests was conducted to determine the efficacy of various "off the shelf" material layups at surface temperatures up to 1300°F in the 8-Ft High Temperature Tunnel at NASA LaRC [111]. Layups consisted of an outer (heatshield) layer, gas barrier, and inner (insulator) layer of various materials and combinations. The combination heatshield and insulator forms the Thermal Protection System (TPS). Results showed that the heavier outer fabrics had the best durability and an aerogel-based insulator performed the best out of the configurations tested. More tests with different materials, different layups, and different test conditions are planned to further explore the trade space. The end goal of this effort is to determine the most effective and lightweight material layup to shield an inflated bladder, such as a stacked toroid, during hypersonic entry. This is in contrast to the work performed in the 1960's, which focused on a single

structural material with high-temperature capability and was more suited for a supersonic application. These upcoming tests will determine the layup used for the next IRVE launch (IRVE-3), which will launch in Spring 2012.

For supersonic IAD applications, strong woven materials with moderate thermal characteristics such as Kevlar [112] and Vectran have emerged as favored materials. Silicon oil or urethane-based coatings are regularly applied to these materials to reduce porosity. Predicting the response of such materials under aerodynamic loads with finite element analysis codes is difficult given the lack of textile material property knowledge. Hutchings recently obtained experimental data for several orthotropic textile materials for use in finite element models [113] with application to both supersonic and hypersonic IADs.

## 10. CONCLUDING REMARKS

IADs have a history spanning 50 years consisting of extensive design, ground testing, computational analyses, and flight testing. Their utility has been demonstrated on numerous occasions in system studies of human robotic missions and planetary probe missions at destinations like Earth, Mars, Neptune, and Titan. The motivation for IAD development ceased after the Viking-era development programs, and now engineers are faced with rediscovering many of the lessons learned by the true pioneers of this technology. Investments by NASA and other entities in the last 10 years have revealed the tension cone, isotensoid, and stacked torus as most probable configurations for application to a planetary probe mission.

Technical discussions of the major IAD disciplines were presented in this survey for trailing and attached configurations of the candidate decelerators, including aerodynamics, stability, aerothermodynamics, structures, inflation, and materials.

The trailing isotensoid has lower drag than its attached counterpart due to the momentum deficit in the wake of the leading body. Unlike the attached configurations, the drag performance of the isotensoid increases as Mach number decreases toward the transonic regime. However, experimental results have shown that the aerothermodynamic environment of an IAD in the wake is far more benign than that of the leading body. Among attached IAD configurations, the tension cone has demonstrated 35% higher supersonic and hypersonic drag than the isotensoid due to differences in aerodynamic shape and burble fence inefficiencies. This result suggests that a burble fence should not be included in isotensoid designs intended only for speeds higher than transonic. Both configurations have higher drag than their trailing counterparts. Embedded shock formation for hypersonic operations of the tension cone remains a concern. Recent research in IAD material technology has revealed several promising layups that may be able to combat the aerothermodynamic environments of interest.

Aerodynamic analysis of these flexible decelerators is not complete unless a rigorous aeroelastic analysis is also performed to incorporate the effects of structural deformation. Structural design and analysis of IADs generally begins by assuming linear theory to determine the shapes and stresses necessary to maintain biaxial tension against a known aerodynamic load. Engineers who design the tension cone and isotensoid rely on these techniques to develop decelerators that minimize fabric wrinkling. The stacked-toroid blunted cone, constructed of multiple concentric toroidal bladders, is a more structurally robust shape than both the isotensoid and tension cone but requires more fabric than the alternatives.

Mass estimation of IADs remains an immature field in large part due to the lack of historical precedence for constructing full-scale flight articles. The same linear theories used for structural design are also useful for mass estimation since one can deduce system mass from computations of fabric acreage and meridional cord length. Trailing SIAD configurations suffer a large mass penalty for the extra towline, which must be sized to carry the entire aerodynamic force. Minimizing towline length can reduce this penalty, but comes at the expense of lower SIAD drag due to the large momentum deficit in the near wake flow field. Among the considered SIAD geometries, the attached tension cone and attached isotensoid likely represent the lowest mass solutions. Future HIAD mass estimation methods must account for thermal effects and accommodate non-uniform material properties.

## REFERENCES


[1] Cruz, J.R., Lingard, J.S., "Aerodynamic Decelerators for Planetary Exploration: Past, Present, and Future," AIAA Guidance, Navigation, and Control Conference and Exhibit, AIAA 2006-6792, August 2006.

[2] Lyons, D.T., Johnson W.R., "Ballute Aerocapture Trajectories at Neptune," AIAA Atmospheric Flight Mechanics Conference and Exhibit, AIAA 2004-5181, August 2004.

[3] Medlock, K.L.G., Ayoubi, M.A., Longuski, J.M., Lyons, D.T., "Analytic Solutions for Aerocapture, Descent, and Landing Trajectories for Dual-Use Ballute Systems," AIAA/AAS Astrodynamics Specialist Conference and Exhibit, AIAA 2006-6026, August 2006.

[4] Reza, S. Hund, R., Kustas, F., Willcockson, W., Songer, J., "Aerocapture Inflatable Decelerator (AID) for Planetary Entry," 19th AIAA Aerodynamic Decelerator Systems Technology Conference and Seminar, AIAA 2007-2516, May 2007.

[5] Rohrschneider, R.R., Braun, R.D., "Survey of Ballute Technology for Aerocapture," Journal of Spacecraft and Rockets, Vol. 44, No. 1, January 2007.

[6] Rohrschneider, R.R., Braun, R.D., "Static Aeroelastic Analysis of Thin-Film Clamped Ballute for Titan Aerocapture," Journal of Spacecraft and Rockets, Vol. 45, No. 4, July 2008.

[7] Clark, I.G., Braun, R.D., "Ballute Entry Systems for Lunar Return and Low-Earth-Orbit Return Missions," Journal of Spacecraft and Rockets, Vol. 45, No. 3, May 2008.

[8] Clark, I.G., Hutchings, A.L., Tanner, C.L., Braun, R.D., "Supersonic Inflatable Aerodynamic Decelerators for Use on Future Robotic Missions to Mars," Journal of Spacecraft and Rockets, Vol. 46, No. 2, March 2009.

[9] Steinfeldt, B.A., Theisinger, J.E., Korzun, A.M., Clark, I.G., Grant, M.J., Braun, R.D., "High Mass Mars Entry, Descent, and Landing Architecture Assessment," AIAA Space 2009 Conference & Exposition, AIAA 2009-6684, September 2009.

[10] Drake, B.G., "Human Exploration of Mars Design Reference Architecture (DRA) 5.0," NASA Special Report, NASA SP-2009-566, July 2009.

[11] McShera, J.T., Keyes, J.W., "Wind-Tunnel Investigations of a Balloon as a Towed Decelerator at Mach Numbers from 1.47 to 2.50," NASA Technical Note, NASA TN-D-919, August 1961.

[12] Charczenko, N., McSheara, J.T., "Aerodynamic Characteristics of Towed Cones Used as Decelerators at Mach numbers from 1.57 to 4.65," NASA Technical Note, NASA TN-D-994, December 1961.

[13] Nebiker, F.R., "Feasibility Study of an Inflatable Type Stabilization and Deceleration System for High-Altitude and High-Speed Recovery," Goodyear Aircraft Corporation, WADD TR-60-182, December 1961.

[14] Kayser, L.D., "Pressure Distribution, Heat Transfer, and Drag Tests on the Goodyear Ballute at Mach 10," Arnold Engineering Development Center, AEDC TDR-62-39, March 1962.

[15] Alexander, W.C., "Investigation to Determine the Feasibility of Using Inflatable Balloon Type Drag Devices for Recovery Applications in the Transonic, Supersonic, and Hypersonic Flight Regime Part II: Mach 4 to Mach 10 Feasibility Investigation," Flight Accessories Laboratory Technical Report, ASD TDR-62-702, December 1962.

[16] McShera Jr., J.T., "Aerodynamic Drag and Stability Characteristics of Towed Inflatable Decelerators at Supersonic Speeds," NASA Technical Note, NASA TN-D-1601, March 1963

[17] Charczenko, N., "Aerodynamic Characteristics of Towed Spheres, Conical Rings, and Cones Used as Decelerators at Mach Numbers from 1.57 to 4.65, NASA Technical Note, NASA TN-D-1789, April 1963.

[18] White, W.E., Riddle, C.D., "An Investigation of the Deployment Characteristics and Drag Effectiveness of the Gemini Personnel Decelerator at Subsonic and Supersonic Speeds, Phase II," ARO Inc. Contractor Report, December 1963.

[19] Nebiker, F.R., "Development of a Ballute Recovery System for Mach 10 Flight and Its Practical Applications," Goodyear Aerospace Corporation Contractor Report, GER-11467A, August 1964.

[20] Bell, D.R., "Pressure Measurements on the Rigid Model of a Balloon Decelerator the Wake of a Simulated Missile Payload at Mach Numbers 1.5 to 6.0," ARO Inc. Technical Report, AEDC TDR-64-65, April 1964.

[21] Bernot, P.T., "Longitudinal Stability Characteristics of Several Proposed Planetary Entry Vehicles at Mach 6.73," NASA Technical Note, NASA TN-D-2785, April 1965.

[22] Deitering, J.S., Hilliard, E.E., "Wind Tunnel Investigation of Flexible Aerodynamic Decelerator Characteristics at Mach Numbers 1.5 to 6.0," ARO Inc. Technical Report, AEDC TDR-65-110, June 1965.

[23] Nebiker, F.R., "Aerodynamic Deployable Decelerator Performance-Evaluation Program," Goodyear Aerospace Corporation Technical Report, AFFDL TR-65-27, August 1965.

[24] Robinson, J.C., Jordan, A.W., "Exploratory Experimental Aerodynamic Investigation of Tension Shell Shapes at Mach 7," NASA Technical Note, NASA TN-D-2994, September 1965.

[25] Graham Jr., J.J., "Development of Ballute for Retardation of Arcas Rocketsondes," Goodyear Aerospace Corporation Contractor Report, AFCRL 65-877, December 1965.

[26] Stroud, W.J., Zender, G.W., "Experimental Investigation to Determine Utility of Tension Shell Concept," NASA Technical Memorandum, NASA TM-X-1211, March 1966.

[27] Creel Jr., T.R., "Longitudinal Aerodynamic Characteristics of a Tension Shell Entry Configuration at Mach 20," NASA Technical Note, NASA TN-D-3541, August 1966.

[28] Turk, R.A., "Pressure Measurements on Rigid Model of Ballute Decelerator at Mach Numbers from 0.56 to 1.96," NASA Technical Note, NASA TN-D-3545, August 1966.

[29] Deveikis, W.D., Sawyer, J.W., "Aerodynamic Characteristics of Tension Shell Shapes at Mach 3.0," NASA Technical Note, NASA TN-D-3633, October 1966.

[30] Harris, C.D., "Transonic Aerodynamic Investigation of Tension Shell and Blunted 100º Conical Shapes for Unmanned Entry Vehicles," NASA Technical Note, NASA TN-D-3700, November 1966.

[31] Ryan, J.E., "Aerodynamic Deceleration from as High as Mach 4.0 for the ALARR (Air Launched Air Recoverable Rocket) Project," Air Force Technical Applications Center, 1966.

[32] Jones, R.A., Bushnell D.M., Hunt, J.L., "Experimental Flow Field and Heat-Transfer Investigation of Several Tension Shell Configurations at a Mach Number of 8," NASA Technical Note, NASA TN-D-3800, January 1967.

[33] Bloetscher, F., "Aerodynamic Deployable Decelerator Performance-Evaluation Program, Phase II," Goodyear Aerospace Corporation Technical Report, AFFDL TR-67-24, June 1967.

[34] Sawyer, J.W., Deveikis, W.D., "Effects of Configuration Modifications on Aerodynamic Characteristics of Tension Shell Shapes at Mach 3.0," NASA Technical Note, NASA TN-D-4080, August 1967.

[35] Nebiker, F.R., "PEPP Ballute Design and Development Final Report," NASA Contractor Report, NASA CR-66585, September 1967.

[36] Kyser, A.C., "Deployment Mechanics for an Inflatable Tension-Cone Decelerator," NASA Contractor Report, NASA CR-929, November 1967.

[37] Walker, B., Weaver, R.W., "Static Aerodynamic Characteristics of Blunted Cones in the Mach-Number Range from 2.2 to 9.5," NASA Technical Report, NASA TR-32-1213, December 1967.

[38] Reichenau, D.E.A., "Investigation of an Attached Inflatable Decelerator System for Drag Augmentation of the Voyager Entry Capsule at Supersonic Speeds," ARO Inc. Technical Report, AEDC TR-68-71, April 1968.

[39] Barton, R.R., "Development of Attached Inflatable Decelerators for Supersonic Applications," NASA Contractor Report, NASA CR-66613, May 1968.

[40] Mikulas Jr., M.M., Bohon, H.L., "Summary of the Development Status of Attached Inflatable Decelerators," AIAA 2nd Aerodynamic Deceleration Systems Conference, AIAA 68-929, September 1968.

[41] Murrow, H.N., McFall Jr., J.C., "Summary of Experimental Results Obtained from the NASA Planetary Entry Parachute Program," AIAA 2nd Aerodynamic Deceleration Systems Conference, AIAA 68-934, September 1968.

[42] Baker, D.C., "Investigation of an Inflatable Decelerator Attached to a 120-deg Conical Entry Capsule at Mach Numbers from 2.55 to 4.40," ARO Inc. Technical Report, AEDC TR-68-227, October 1968.

[43] Graham Jr., J.J., "Ballute Development for Loki-Dart and Arcas Rocketsondes," Goodyear Aerospace Corporation Technical Report, AFCRL 68-0622, November 1968.

[44] Usry, J.W., "Performance of a Towed, 48-Inch-Diameter (121.92-cm) Ballute Decelerator Tested in Free Flight at Mach Numbers from 4.2 to 0.4," NASA Technical Note, NASA TN-D-4943, February 1969.

[45] Davenport, E.E., "Static Longitudinal Aerodynamic Characteristics of Some Supersonic Decelerator Models at Mach Numbers of 2.30 and 4.63." NASA Technical Note, NASA TN-D-5219, May 1969.

[46] Mayhue, R.J., Eckstrom, C.V., "Flight-Test Results from Supersonic Deployment of an 18-Foot-Diameter (5.49-meter) Towed Ballute Decelerator," NASA Technical Memorandum, NASA TM-X-1773, May 1969.

[47] Baker, D.C., "Investigation of an Attached Inflatable Decelerator with Mechanically Deployed Inlets at Mach Numbers from 2.25 to 4.75," ARO Inc. Technical Report, AEDC TR-69-132, June 1969.

[48] Mikulas Jr., M.M., Bohon, H.L., "Development Status of Attached Inflatable Decelerators," Journal of Spacecraft, Vol. 6, No. 6, June 1969.

[49] Deveikis, W.D., Sawyer, J.W., "Static Aerodynamic Characteristics, Pressure Distributions, and Ram-Air Inflation of Attached Inflatable Decelerator Models at Mach 3.0," NASA Technical Note, NASA TN-D-5816, May 1970.

[50] Miserentino, R., and Bohon, H.L., "Drag Characteristics of Several Towed Decelerator Models at Mach 3," NASA Technical Note, NASA TN-D-5750, May 1970.

[51] Bohon, H.L., Miserentino, R., "Deployment and Performance Characteristics of 5-Foot-Diameter (1.5 m) Attached Inflatable Decelerators from Mach Number 2.2 to 4.4," NASA Technical Note, NASA TN-D-5840, August 1970.

[52] Faurote, G. L., "Design, Fabrication, and Static Testing of Attached Inflatable Decelerator (AID) Models," NASA Contractor Report, NASA CR-111831, 1971.

[53] Bohon, H.L., Miserentino, R., "Attached Inflatable Decelerator (AID) Performance Evaluation and Mission-Application Study," Journal of Spacecraft, Vol. 8, No. 9, September 1971.

[54] Creel, T.R., Miserentino, R., "Aerodynamic Heating at Mach 8 of Attached Inflatable Decelerator Configurations," NASA Technical Memorandum, NASA TM-X-2355, October 1971.

[55] Johnson, B.A., "Design, Fabrication, and Static Testing of First-Stage Attached Inflatable Decelerator (AID) Models," Goodyear Aerospace Corporation Technical Report, GER-15267, 1971.

[56] Faurote, G.L., Burgess, J.L., "Thermal and Stress Analysis of an Attached Inflatable Decelerator (AID) Deployed in the Mars and Earth Atmospheres," Goodyear Aerospace Corporation Technical Report, GER-14939, 1971.

[57] Willis, C.M., Mikulas Jr., M.M., "Static Structural Tests of a 1.5-Meter-Diameter Fabric Attached Inflatable Decelerator," NASA Technical Note, NASA TN-D-6929, October 1972.

[58] Evors, R.A., "Evaluation of a Ballute Retarder System for the MK 82 Bomb," Armament Development and Test Center Technical Report, ADTC TR-73-31, May 1973.

[59] Pyle, J.S., Phelps, J.R., Baron, R.S., "Performance of a Ballute Decelerator Towed Behind a Jet Airplane," NASA Technical Memorandum, NASA TM-X-56019, December 1973.

[60] Bohon, H.L., Sawyer, J.W., "Deployment and Performance Characteristics of 1.5-Meter Supersonic Attached Inflatable Decelerators," NASA Technical Note, NASA TN-D-7550, July 1974.

[61] Keville, J.F., "Semi-Rigid or Non-Rigid Structures for Re-Entry Applications, Part I: Evaluation and Design," Air Force Materials Laboratory Technical Report, AFML TR-67-310, September 1967.

[62] Keville, J.F., "Semi-Rigid or Non-Rigid Structures for Re-Entry Applications, Part II: Fabrication and Test," Air Force Materials Laboratory Technical Report, AFML TR-67-310, September 1967.

[63] Keville, J.F., "Semi-Rigid or Non-Rigid Structures for Re-Entry Applications, Part III: Appendices," Air Force Materials Laboratory Technical Report, AFML TR-67-310, September 1967.

[64] Braun, R.D., Manning, R.M., "Mars Exploration Entry, Descent, and Landing Challenges," Journal of Spacecraft and Rockets, Vol. 44, No. 2, March 2007.

[65] Leonard, R.W., Brooks, G.W., McComb Jr., H.G., "Structural Considerations of Inflatable Reentry Vehicles," NASA Technical Note, NASA TN-D-457, September 1960.

[66] Fallon II, E.J., "Supersonic Stabilization and Deceleration: Ballutes Revisited," AIAA 95-1584-CP, 1995.

[67] Author's conversation with Loral Space and Communications Company.

[68] Graham, W.A., "MK 82 Ballute Retarder System Updated for Advanced Weapons Program," 16th Aerodynamic Decelerator Systems Technology Conference and Seminar, AIAA 2001-2039, May 2001.

[69] Iannotta, B. "Future Mars Craft Inspires High-Tech Spy Plane," Space.com Online Publication, Posted 31 October 2007.

[70] Kustas, F.M., Rawal, S.P., Willcockson, W.H., Edquist, C.T., Thornton, J.M., Sandy, C., "Inflatable Decelerator Ballute for Planetary Exploration Spacecraft," AIAA 2000-1795, 2000.

[71] Walther, S. et al., "New Space Application Opportunities based on the Inflatable Reentry & Descent Technology (IRDT)," AIAA/ICAS International Air and Space Symposium and Exposition: The Next 100 Years, AIAA 2003-2839, July 2003.

[72] Miller, K.L., Gulick, D., Lewis, J., Trochman, B., Stein, J., Lyons, D.T., Wilmoth, R.G., "Trailing Ballute Aerocapture: Concept and Feasibility Assessment," 39th AIAA/ASME/SAE/ASEE Joint Propulsion Conference and Exhibit, AIAA 2003-4655.

[73] Hughes, S.J., Dillman, R.A., Starr, B.R., Stephan, R.A., Lindell, M.C., Player, C.J., Cheatwood, F.M., "Inflatable Re-entry Vehicle Experiment (IRVE) Design Overview," 18th AIAA Aerodynamic Decelerator Systems Technology Conference and Seminar, AIAA 2005-1636, September 2005.

[74] Richardson, E.H., Munk, M.M., James, B.F., Moon, S.A., "Review of NASA In-Space Propulsion Technology Program Inflatable Decelerator Investments," 18th AIAA Aerodynamic Decelerator Systems Technology Conference and Seminar, AIAA 2005-1603, July 2005.

[75] Masciarelli, J.P., Lin, J.K.H., Ware, J.S., Rohrschneider, R.R., Braun, R.D., Bartels, R.E., Moses, R.W., Hall, J.L., "Ultra Lightweight Ballutes for Return to Earth from the Moon," 47th AIAA/ASME/ASCE/AHS/ASC Structures, Structural Dynamics, and Materials Conference, AIAA 2006-1698, May 2006.

[76] Player, C., "Inflatable Aerodynamic Decelerators Technology Development," Fundamental Aeronautics 2007 Annual Meeting Conference Proceedings, October 2007.

[77] Braun, R.D., "Strengthening NASA's Technology Development Programs," Written statement to the U.S. House of Representatives Subcommittee on Space and Aeronautics of the Science and Technology Committee, 22 October 2009.

[78] Nerem, R.M., "An Approximate Method for Including the Effect of the Inviscid Wake on the Pressure Distribution on a Ballute-Type Decelerator," Goodyear Aerospace Corporation Engineering Procedure, GER-11824, November 1964.

[79] Jaremenko, I.M., "Wakes, their Structure and Influence Upon Aerodynamic Decelerators," NASA Contractor Report, NASA CR-748, April 1967.

[80] Jaremenko, I.M., "BALLUTE Characteristics in the 0.1 to 10 Mach Number Speed Regime," Journal of Spacecraft, Vol. 4, No. 8., August 1967.

[81] Moss, J.N., Mitcheltree, R.A., Wilmoth, R.G., "Hypersonic Blunt Body Wake Computations using DSMC and Navier-Stokes Solvers," AIAA 28th Thermophysics Conference, AIAA 93-2807, July 1993

[82] Zhong, J., Ozawa, T., Levin, D.A., "Comparison of High-Altitude Hypersonic Wake Flows of Slender and Blunt Bodies," AIAA Journal, Vol. 46, No.1, January 2008.

[83] Anderson, M. S., Robinson, J. C., Bush, H. G., Fralich, R. W., "A Tension Shell Structure for Application to Entry Vehicles," NASA Technical Note, NASA TN D-2675, 1965.

[84] Sawyer, J.W., "Effects of Pressure Distributions on Bluff Tension-Shell Shapes," NASA Technical Note, NASA TN-D-5636, February 1970.

[85] Clark, I.G., "Aerodynamic Design, Analysis, and Validation of a Supersonic Inflatable Decelerator," Georgia Tech PhD Thesis, August 2009.

[86] Steinberg, S., Siemers III, P.M., Slayman, R.G., "Development of the Viking Parachute Configuration by Wind Tunnel Investigation," AIAA 4th Aerodynamic Deceleration Systems Conference, AIAA 73-454, May 1973.

[87] Alexander, W. C., Lau, R. A., "State-of-the-Art Study for High-Speed Deceleration and Stabilization Devices," GER-12616, 1966.

[88] Kyriss, C.L., Rie, H., "Theoretical Investigation of Entry Vehicle Stability in the Mars Atmosphere," Journal of Spacecraft, Vol. 4, No. 2, February 1967.

[89] Yates, L.A., "Analysis of Data from Ballistic Range Tests of PAIDAE Vehicles," Final Report for NASA LaRC, November 2007.

[90] Sawyer, J.W., Whitcomb, C.F., "Subsonic and Transonic Pressure Distributions around a Bluff Afterbody in the Wake of a 120º Cone for Various Separation Distances," NASA Technical Note, NASA TN-D-6569, November 1971.

[91] Hornung, H., "Hypersonic Flow Over Bodies in Tandem," Shock Waves, Vol. 11, No. 6, pp. 441–445, 2002.

[92] Gnoffo, P., "Computational Aerothermodynamics in Aeroassist Applications," Journal of Spacecraft and Rockets, Vol. 40, No. 3, pp. 305–312, 2003.

[93] Gnoffo, P. and Anderson, B., "Computational Analysis of Towed Ballute Interactions," AIAA Paper 2002-2997, 8th AIAA/ASME Joint Thermophysics and Heat Transfer Conference, Saint Louis, MO, June 2002.

[94] Gnoffo, P. A., et al., "Aerothermodynamic Analyses of Towed Ballutes", AIAA/ASME Joint Thermophysics and Heat Transfer Conference, AIAA 2006-3771, May 2006.

[95] Rasheed, A., Fujii, K., Hornung, H., and Hall, J., "Experimental Investigation of the Flow Over a Toroidal Aerocapture Ballute," AIAA Paper 2001-2460, 19th AIAA Applied Aerodynamics Conference, Anaheim, CA, June 2001.

[96] McIntyre, T., Lourel, I., Eichmann, T., Morgan, R., Jacobs, P., and Bishop, A., "Experimental Expansion Tube Study of the Flow Over a Toroidal Ballute," Journal of Spacecraft and Rockets, Vol. 41, Bo. 5, pp. 716–725, 2004.

[97] Houtz, N. E., "Optimization of Inflatable Drag Devices by Isotensoid Design," AIAA Annual Meeting, AIAA-1964-437, 1964.

[98] Clark, I. G., Hutchings, A. L., Tanner, C. L., Braun, R. D., "Supersonic Inflatable Aerodynamic Decelerators for Use on Future Robotic Missions to Mars," IEEE Aerospace Conference, IEEEAC paper #1419, 2008.

[99] Brown, G. J., Lingard, J. S., Darley, M. G., Underwood, J. C., "Inflatable Aerocapture Decelerators for Mars Orbiters," AIAA Aerodynamic Decelerator Systems Technology Conference and Seminar, AIAA-2007-2543, 2007.

[100] Brown, G. J., "Estimating Minimum Inflation Pressure for Inflatable Aerodynamic Decelerators," AIAA Aerodynamic Decelerator Systems Technology Conference and Seminar, AIAA-2009-2970, 2009.

[101] Lindell, M.C., Hughes, M.C., Dixon, M., Willey, C.E., "Structural Analysis and Testing of the Inflatable Re-entry Vehicle Experiment (IRVE)," 47th AIAA/ASME/ASCE/AHS/ASC Structures, Structural Dynamics, and Materials Conference, AIAA 2006-1699, May 2006.

[102] Park, C., "Theory of Idealized Two-Dimensional Ballute in Newtonian Hypersonic Flow," Journal of Spacecraft and Rockets, Vol. 25, No. 3, p. 986, May 1988.

[103] Mosseev, Y. "The Decelerator Pitch-Dependent Performances Prediction Based on 3D Aeroelastic Analysis," AIAA 97-1717, CEAS/AIAA Aerodynamic Decelerator Systems Technology Conference, June 1999.

[104] Karagiozis, K., Cirak, F., Kamakoti, R., Pantano, C., Gidzak, V., Nompelis, I., Stein, K., Candler, G., "Computational Fluid-Structure Interaction Methods for Simulation of Inflatable Aerodynamic Decelerators," AIAA 2009-2968, AIAA Aerodynamic Decelerator Systems Technology Conference and Seminar, May 2009.

[105] Gilmanov, A., Acharya, S., Gilmanov, T., "Flow-Structure Interaction Simulations for Ballutes in Supersonic Flow," AIAA 2009-2906, AIAA Aerodynamic Decelerator Systems Technology Conference and Seminar, May 2009.

[106] Weeks, G. E., "Buckling of a Pressurized Toroidal Ring Under Uniform External Loading," NASA Technical Note, NASA TN D-4124, 1967.

[107] Anderson, M. S., Bohon, H.L., "A Structural Merit Function for Aerodynamic Decelerators," NASA Technical Note, NASA TN-D-5535, November 1969.

[108] Brown, G.J., "Hypercone Inflatable Supersonic Decelerator," 17th AIAA Aerodynamic Decelerator Systems Technology Conference and Seminar, AIAA 2004-2167, May 2003.

[109] Musil, J.L., "Study of Expandable, Terminal Decelerators for Mars Atmosphere Entry: Volume I," Goodyear Aerospace Corporation Contractor Report, GER-12842 Rev A, October 1966.

[110] Musil, J.L., "Study of Expandable, Terminal Decelerators for Mars Atmosphere Entry: Volume II," Goodyear Aerospace Corporation Contractor Report, GER-12842, October 1966.

[111] Hughes, S. J., Ware, J. S., Del Corso, J. A., Lugo, R. A., "Deployable Aeroshell Flexible Thermal Protection System Testing," AIAA Aerodynamic Decelerator Systems Technology Conference and Seminar, AIAA-2009-2926, 2009.

[112] Clark, I. G., Cruz, J. R., Hughes, M. F., Ware, J. S., Madlangbayan, A., Braun, R. D., "Aerodynamic and Aeroelastic Characteristics of a Tension Cone Inflatable Aerodynamic Decelerator," AIAA Aerodynamic Decelerator Systems Technology Conference and Seminar, AIAA 2009-2967, 2009.

[113] Hutchings, A.L., Braun, R.D., Masuyama, K., Welch, J.V., "Experimental Determination of Material Properties for Inflatable Aeroshell Structures," 20th AIAA Aerodynamic Decelerator Systems Technology Conference and Seminar, AIAA 2009-2949, May 2009.

## BIOGRAPHIES

***Brandon Smith*** *is a graduate research assistant in the Space Systems Design Laboratory at the Georgia Institute of Technology. Brandon has previously interned at NASA Langley Research Center, NASA Ames Research Center, Andrews Space, and Sikorsky Aircraft Corporation. Brandon is a current member of the flight dynamics team for the Inflatable Reentry Vehicle Experiment. His current research focuses on the design, testing, and integration of hypersonic inflatable aerodynamic decelerators. He has a BS in Aerospace Engineering from Georgia Tech.*

***Chris Tanner*** *is a PhD student in the Space Systems Design Laboratory at the Georgia Institute of Technology. Chris has previously worked as a cooperative education student at NASA Johnson Space Center and as an intern at the Aerospace Corporation. He has participated in systems studies ranging from Mars surface systems to hypersonic airbreathing vehicles to Mars entry vehicles. His current research focuses on the experimental and computational analysis of inflatable aerodynamic decelerators. He has a BS and MS in Aerospace Engineering from Georgia Tech.*

***Robert Braun*** *is an Associate Professor in the Daniel Guggenheim School of Aerospace Engineering at the Georgia Institute of Technology. As Director of Georgia Tech' s Space Systems Design Laboratory, he leads a research program focused on the design of advanced flight systems and technologies for planetary exploration. He is responsible for undergraduate and graduate level instruction in the areas of space systems design, astrodynamics and planetary entry. Prior to coming to Georgia Tech, Dr. Braun worked at NASA Langley Research Center for sixteen years where he contributed to the design, development, test, and operation of several robotic space flight systems. Dr. Braun is an AIAA Fellow and the principal author or co-author of over 175 technical publications in the fields of planetary exploration, atmospheric entry, multidisciplinary design optimization, and systems engineering.*

***Milad Mahzari*** *is a graduate research assistant in the Space Systems Design Laboratory at the Georgia Institute of Technology. He has previously interned at NASA Ames Research Center where he participated in the design of a reentry system for the recovery of the in space Cubesat experiments. His current research is related to thermal protection system performance and heating reconstruction using flight data. He has a BS in Aerospace Engineering from Georgia Tech.*

***Ian Clark*** *is an employee of the Jet Propulsion Laboratory and recipient of his PhD from the Georgia Institute of Technology, where he also received his BS and MS. Ian's current research involves developing and maturing inflatable aerodynamic decelerators for use during atmospheric entry. As part of this research, Dr. Clark has worked on conceptual IAD system design, entry flight mechanics trades, and the development of fluid- structure interaction codes capable of predicting the behavior of flexible decelerators.*

***Neil Cheatwood*** *has played key roles in NASA's planetary atmospheric flight programs. He is a nationally recognized expert in aerosciences and flight mechanics for planetary entry systems. He is the Principle Investigator for the Mars Entry, Descent, and Landing Instrumentation (MEDLI) project. He leads LaRC efforts to develop inflatable aeroshell technologies. He is the Principle Investigator for NASA LaRC's Inflatable Reentry Vehicle Experiment (IRVE), as well as the follow-on Program to Advance Inflatable Decelerators for Atmospheric Entry. Dr. Cheatwood was responsible for the entry aerodynamic databases for the Stardust, Mars Microprobe, Genesis, and Mars Exploration Rovers missions. He has also contributed to the Mars Global Surveyor and Mars Sample Return flight projects. Dr. Cheatwood is an AIAA Associate Fellow and the principle author or co-author of over 60 technical publications in the fields of fluid dynamics, atmospheric entry, and systems engineering.*